13th World Conference on Earthquake Engineering
Vancouver, B.C., Canada
August 1-6, 2004
Paper No. 1877

DYNAMIC COLLAPSE OF CFT-FRAME UNDER EXTREMELY STRONG GROUND MOTION

Motoo SAISHO[1]

SUMMARY

Collapse analysis method of concrete filled steel tube frame (CFT frame) under extremely strong ground motion is obtained by the use of the non-dimensional restoring force model of CFT column which is composed of the Tri-linear model and the Clough model and can predict the fracture failure of it. Multi-story CFT frames are designed and the collapse behaviors of them are calculated by the presented analysis method. From the results it is ascertained that the proposed collapse analysis method is useful to calculate multi-story CFT frames. It is also shown that the local buckling and the crack of steel tube of CFT column are closely related to the collapse of CFT frame and they are the basic factors of CFT frame design against strong ground motion.

1. INTRODUCTION

The basic object of earthquake resistant design of building structure is to prevent the collapse of frame and the injury to person which have been observed in the recent severe earthquakes. To design building on the basis of the ultimate state and to prevent the collapse of building, the collapse behavior of building under extremely strong ground motion is required to be analyzed. From this reason the analysis method of dynamic collapse is obtained in this study and some calculations of concrete filled steel tube frame (CFT frame) under extremely strong ground motion are carried out. The damage of CFT frame is also investigated in relation with the collapse behavior and the earthquake resistant design of frame.

2. EQUATION OF MOTION AND MULTI-STORY FRAME MODEL

2.1 Multi-story frame model

In the dynamic collapse analysis of frame, the multi-story plane frame is assumed to be composed of the rigid panel zones of member connection and the axially elastic members with elastic-plastic hinges at the

[1] Professor, Kumamoto Univ., Kumamoto, Japan. Email: saisho@gpo.kumamoto-u.ac.jp

both ends as explained in Fig.1. The mass of frame is concentrated in every panel zone and distributed uniformly in it. Accordingly the deformation of frame can be expressed only by the rotation (θ_i, i: number of panel zone), the horizontal displacement (u_i) and the vertical displacement (w_i) of every rigid panel zone.

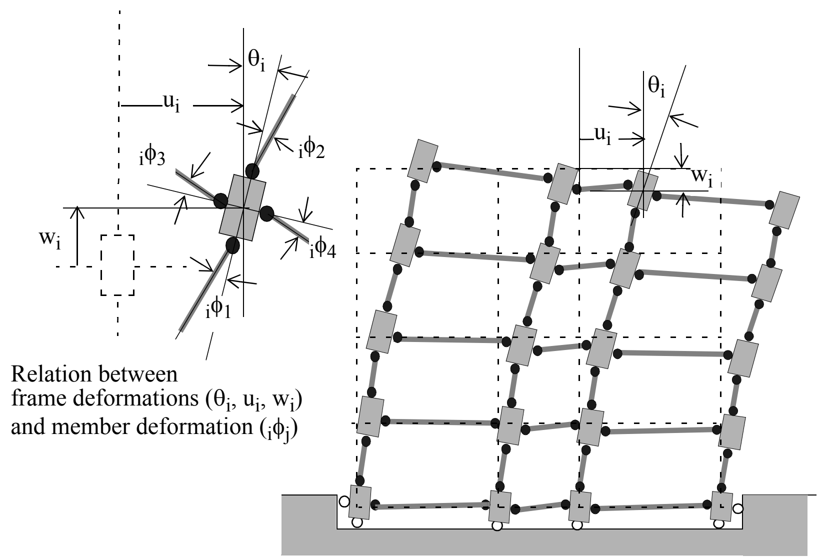

Fig.1 Frame model for numerical analysis

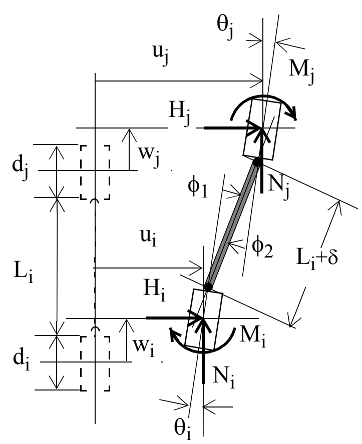

Fig.2 Column model

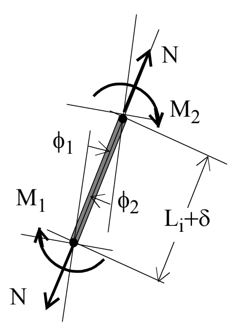

Fig.3 Bending moment and axial force of elastic-plastic hinge

2.2 Stiffness matrix and equation of motion

The relations between the end forces (M_1, M_2, N) and deformations (ϕ_1, ϕ_2, δ) of column shown in Fig.3 are expressed by Eq.(1).

$$\{\Delta s\}=[k_0]\{\Delta e\} \tag{1}$$

in which $\{\Delta s\}=[\Delta M_1\ \Delta M_2\ \Delta N]^T$, $\{\Delta e\}=[\Delta\phi_1\ \Delta\phi_2\ \Delta\delta]^T$ and Δ means the increment. $[k_0]$ is the diagonal matrix and the diagonal elements (k_1, k_2, k_3) are the rotational stiffness of elastic-plastic hinge ($k_n=\Delta M_n/\Delta\phi_n$, n=1,2) and the elastic axial stiffness of column (k_3). The rotational stiffness is decided by the restoring force characteristics of the elastic-plastic hinge which are expressed by the restoring force model explained in the next section.

From Eq.(1), the relations between the incremental forces $\{\Delta f\}$ and deformations $\{\Delta d\}$ at the center of rigid panel zone (Fig.2) are derived.

$$\{\Delta f\}=[k]\{\Delta d\}$$
$$[k]=[p]+[t]^T[k_0][t] \qquad (2)$$

in which $\{f\}=[M_i\ M_j\ H_i\ H_j\ N_i\ N_j]^T$, $\{d\}=[\theta_i\ \theta_j\ u_i\ u_j\ w_i\ w_j]^T$, [p]: the matrix to express the P-Δ effect of column, [t]: the transfer matrix from $\{\Delta e\}$ to $\{\Delta d\}$. To analyze the large deformation and the collapse behavior of frame the elements of [p] and [t] are expressed strictly without neglecting any small components of them. The $\{\Delta f\}$-$\{\Delta d\}$ relation of beam can be also obtained from Eq.(2) by exchanging the horizontal components for the vertical components of force and deformation.

According to the equilibrium condition of loads and end-forces of member and the continuity conditions between the rigid panel displacements and the member deformations, the relation between the incremental loads $\{\Delta F\}$ and incremental deformations $\{\Delta D\}$ of frame is obtained.

$$\{\Delta F\}=[K]\{\Delta D\} \qquad (3)$$

in which $\{\Delta F\}=[\ldots\ \Delta\overline{M}_i\ \ldots\Delta\overline{H}_i\ \ldots\ \Delta\overline{N}_i\ \ldots\ ]^T$, $\{\Delta D\}=[\ldots\Delta\theta_i\ \ldots\Delta u_i\ \ \ldots\ \Delta w_i\ \ldots\ ]^T$ and $\overline{M}_i$, $\overline{H}_i$, $\overline{N}_i$ are the loads working at the center of rigid panel zone. [K] is the tangent stiffness matrix of multi-story frame. By the use of the tangent stiffness matrix [K] mentioned above, the equation of motion of multi-story frame can be expressed by Eq.(4)

$$[M]\{\ddot{D}\}+[C]\{\dot{D}\}+[K]\{D\}=-[M]\{1\}\ddot{D}_g \qquad (4)$$

in which [M]: the mass matrix, [C]: the viscous damping matrix, $\{\ddot{D}_g\}$: the acceleration of ground motion, the dot means the differentiation with time.

To decide the mass matrix [M] and the damping matrix [C] in Eq.(4), the following conditions of frame are also introduced.

i) The mass of frame is concentrated in every rigid panel zone and the rotational inertia of it is determined by assuming the mass in the panel zone distributes uniformly.

ii) The viscous damping of frame is expressed by the Rayleigh damping in which the damping ratios of the first mode (h_1) and the second mode (h_2) are assumed to be h_1=0.02, h_2=0.02.

3. RESTORING FORCE MODEL OF CFT-COLUMN AND H-SECTION BEAM

3.1 Restoring force model of CFT column

The restoring force model of elastic-plastic hinge is obtained on the basis of the dynamic loading test of CFT column[1)-3)]. Fig.4 shows how to define the restoring force (M) and the deformation (ϕ) by the horizontal load (H), the axial load (N) and the the column-end deflection (δ_c) of test result.

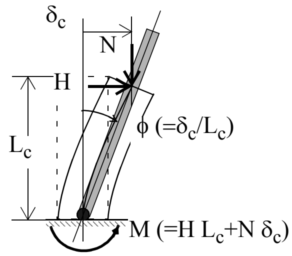

Fig.4 Bending restoring force (M) and deformation (ϕ) defined by test results (H, N, δ_c)

The load deformation relations of test result are in Fig.5 in which ϕ_u=M_u/K_o (M_u: ultimate bending strength, K_o: initial stiffness of elastic-plastic hinge). Fig.5(A) is the load deformation relation in the range of small deformation until the steel tube buckles locally. Fig.5(B) also shows the load deformation relation of the same specimen after the local buckling of steel tube. Until the local buckling of steel tube the non-dimensional restoring force characteristics of CFT column (M/M_u) are spindle-shaped and approximated by the Tri-linear model as shown in Fig.5(A) with thin lines. The skeleton curve of the Tri-linear model explained in Fig.6 is defined by the restoring force characteristics of M_y, M_u, K_o (M_y: yield strength). After the steel tube buckles locally the stiffness of CFT column deteriorates gradually and the non-dimensional restoring force characteristics are approximated by the modified Clough model[4] (Clough model) as shown in Fig.5(B) with thin lines. The skeleton curve of the Clough model explained in Fig.7 is assumed to be expressed only by the restoring force characteristics of K_o, M_u. Under alternating repeated load, the stiffness of CFT column in the unloading process degrades with the cyclic loading and assumed to be expressed by K_r (=$K_0/\mu_m^{0.5}$, μ_m: the maximum ductility factor).

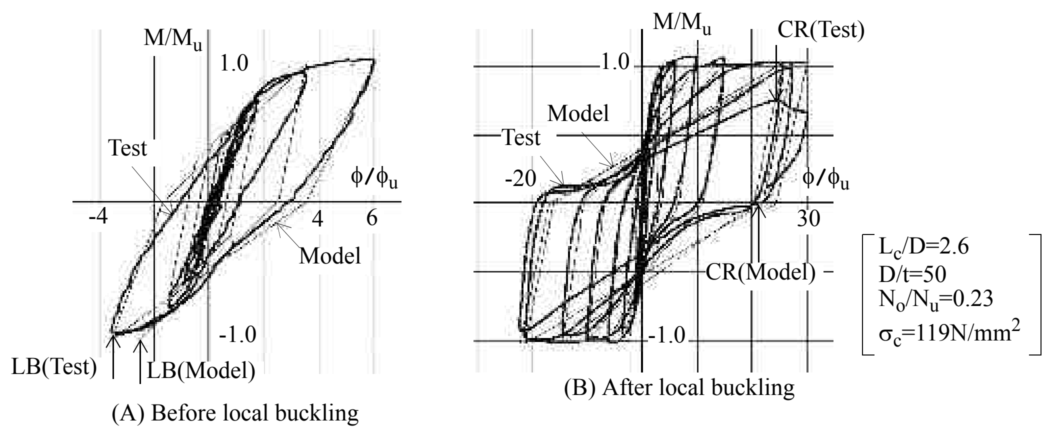

Fig.5 Load deformation relation of CFT column test and the restoring force model (LB: Local buckling, CR: Steel tube crack, L_c/D: Aspect ratio, N_o/N_u: Axial force ratio, σ_c: Concrete strength)

According to these results the non-dimensional restoring force (M/M_u) of CFT column until the local buckling of steel tube is approximated by the Tri-linear model whose skeleton curve is defined in Fig.6 and after the local buckling of steel tube it is expressed by the Clough model whose skeleton curve is the Bi-linear model as shown in Fig.7. The stiffness ratios in the plastic range in Fig.6 and Fig.7 are given as K_1/K_0=0.2, K_2/K_0=0.001 which are approximated on the basis of the test result[1)-3)].

The restoring force model mentioned above is defined by the non-dimensional restoring force (M/M_u) in which the ultimate bending strength M_u changes at every instance according to the varying axial force of CFT column. From this reason the restoring force model presented here is also effective for the CFT column under varying axial force.

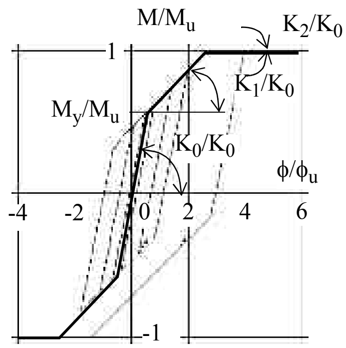

(K_1/K_0=0.2, K_2/K_0=0.001)

Fig.6 Tri-linear model and its skeleton curve

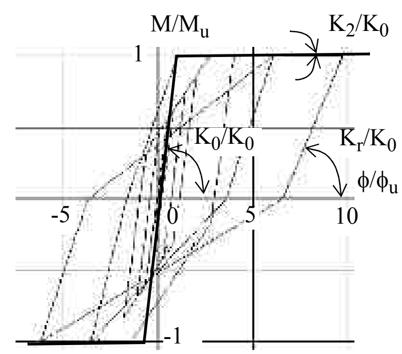

(K_2/K_0=0.001, K_r/K_0:Unloading stiffness)

Fig.7 Clough model and its skeleton curve

3.2 Local buckling and crack of CFT column

The restoring force of CFT column changes extremely due to the steel tube crack and the local buckling of steel tube is closely related to the crack of steel tube. From this reason the local buckling and the crack of steel tube can not be neglected in the restoring force model of CFT column.

The dynamic and repeated loading test of CFT column was carried out and the steel tube crack of CFT column was investigated[1)-2)]. On the basis of the test results it is shown that the steel tube of CFT column cracks when the accumulated plastic strain of steel tube becomes to be the critical value ($\alpha\varepsilon_f$). From this result the crack condition of CFT column is expressed by Eq.(5).

$$\Sigma\varepsilon_{TC}+\Sigma\varepsilon_T = \alpha\varepsilon_f \qquad (5)$$

in which ε_T is the plastic tension strain of steel tube in the tension stress side and ε_{TC} is the plastic strain due to the local buckling deformation of steel tube in the compression stress side as explained in Fig.8. According to Eq.(5) the damage ratio of steel tube crack (D_{cr}) can be expressed by Eq.(6).

$$D_{cr} = (\Sigma\varepsilon_{TC}+\Sigma\varepsilon_T)/\ \alpha\varepsilon_f \qquad (6)$$

As shown in Eq.(5) the local buckling of steel tube is closely related to the steel tube crack. From this reason the condition for steel tube to buckle locally is obtained on the basis of the the upper bound theorem of the limit analysis[5)]. The damage ratio of local buckling (D_{lb}) is decided by the use of critical deformation (δ_{lb}) which corresponds to the CFT column deformation for the steel tube to buckle locally.

$$D_{lb} = (\delta_{PC} - \delta_{PT})/\ \delta_{lb} \qquad (7)$$

in which ($\delta_{PC} - \delta_{PT}$) is the amplitude of plastic deformation of CFT column.

By the use of Eq.(6) and Eq.(7), the local buckling and the crack of steel tube in the restoring force of CFT column mentioned above is decided and it is assumed that the restoring force and the stiffness of CFT column are perfectly lost after the steel tube crack.

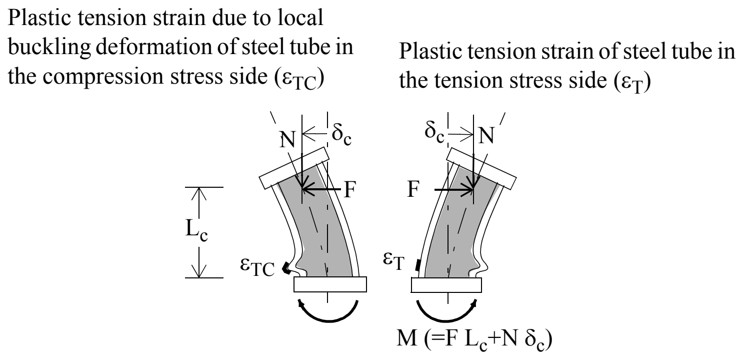

Fig.8 Local buckling deformation and tension strain of steel tube

3.3 Restoring force model of H-section beam

The multi-story CFT frame to be investigated in this study is composed of CFT columns and H-section beams. The H-section beam of multi-story frame is also expressed by the same model of CFT column which is the elastic member with the elastic-plastic hinges at both ends as shown in Fig.1. The restoring force of the elastic-plastic hinge is decided by the Tri-linear model shown in Fig.9 in which the restoring force characteristics are given by the full plastic moment (M_p) and the ultimate bending strength (${}_bM_u$) of H-section beam.

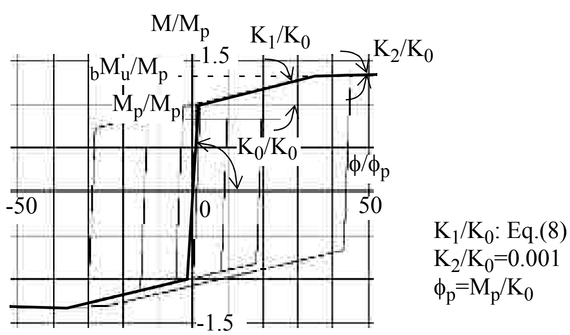

Fig.9 Tri-linear model of H-section beam and its skeleton curve

The strain hardening behavior of H-section beam effects on the seismic response and collapse of CFT frame under strong ground motion. Accordingly the strain hardening of H-section beam in the model can not be neglected. It is given by the value K_1 which is obtained by assuming the H-section beam is approximated by the two-flange section member.

$$\frac{K_1}{K_0} = \frac{1/y - 1}{1.5y(1 - y)(1 + u) - 1} \tag{8}$$

in which $y(=\sigma_y/\sigma_u)$ and $u(=\varepsilon_u/\varepsilon_y)$ mean the yield stress ratio and the ultimate tensile strain ratio respectively.

3.4 Crack of H-section beam

The restoring force and the bending stiffness of H-section beam change significantly due to the crack of it. From this reason the effect of crack on the restoring force of H-section beam must be considered in the seismic analysis of CFT frame.

It is assumed in this study that the crack of H-section beam can be decide on the basis of the Coffin-Manson relationship[6] and the Palmgren-Miner rule[6]. The Coffin-Manson relationship expressed by the strain amplitude (ε_a) of H-section beam under cyclic load is given by Eq.(9).

$$\varepsilon_a = \frac{\sigma_f}{E}(2N_f)^b + \varepsilon_f(2N_f)^c \tag{9}$$

in which N_f: the number of cyclic loading until the crack of H-section beam, σ_f, ε_f: the stress and the plastic strain of H-section beam to crack under monotonic loading, b, c: the constants to be decided according to the material properties (b= -0.085, c= -0.6 are assumed for steel member[6]). The Palmgren-Miner rule to predict the crack under cyclic loading of variable strain amplitude is given by Eq.(10).

$$\sum_j \frac{N_j}{N_{fj}} = 1 \tag{10}$$

in which N_{fj}: the number of loading cycle to crack under the j-th amplitude of strain, N_j: the number of loading cycle under the j-th amplitude of strain.
The strain amplitude (ε_a) at the end of H-section beam can be expressed by the function of beam deformation (ϕ_a) as shown in Eq.(11). To obtain the relation between ε_a and ϕ_a, it is assumed that H-section beam is approximated by the two-flange section member and the stress and plastic strain distribute linearly along the beam axis.

$$\varepsilon_a = \left(\frac{1}{\lambda_b}\right)\frac{1}{\frac{1}{6}(1-y)(2+y)}\phi_a \tag{11}$$

in which λ_b: the slenderness ratio of beam, $y(=\sigma_y/\sigma_u)$: the yield stress ratio. Accordingly the relation between the amplitude of cyclic deformation of H-section beam (ϕ_a) and the number of repeated load until the crack of H-section beam (N_f) is obtained by Eq.(9) and Eq.(11). The obtained number to crack (N_{fj}) is applied to Eq.(10) and N_j/N_{fj} of H-section beam under cyclic load can be decided. From the sum of N_j/N_{fj}, the damage ratio of H-section beam to crack is calculated and the crack damage of H-section beam can be also predicted.

4. DESIGN OF MULTI-STORY CFT FRAME

4.1 Design conditions of CFT frame

The multi-story CFT frames to be calculated in the next section are designed. The multi-story CFT frame investigated in this study is the plane frame and composed of CFT columns and H-section beams. The seismic response and collapse behavior of CFT frame are effected by the column over design factor (r_c) and the strength ratio of filled concrete to steel tube (ρ) beside the well-known base shear strength ratio (C_B)[7]. In consideration of the CFT frame behaviors, the following conditions are assumed in the design of CFT frames.

i) The distribution of story-shear strength ratio (C_i, i: number of story) is strictly corresponding to that of the Japanese design code. The base shear strength ratios (C_B) of the15-story 3-bay frames (F15-3 frame) and the 7-story 3-bay frames (F7-3 frame) are also given according to the design code. They are C_B=0.20 and C_B=0.30 respectively.

ii) The column over design factor (r_c) of every story except the highest story is the same and r_c=1.5.

iii) The strength ratio of filled concrete to steel tube ρ ($=\sigma_c A_c/\sigma_u A_s$, A_c, A_s: sectional areas of concrete and steel tube respectively) effects on the restoring force characteristics of CFT column[1)-3)]. From this reason the strength ratios (ρ) of all CFT columns are assumed to be the same and ρ=1.5.

iv) Every H-section beam of multi-story frame satisfies the relation of $r_x^2/A=4.0$ (r_x: radius of gyration, A: sectional area).

Table-1 F15-3 Frame (σ_c=60N/mm^2)

Story	Steel tube of CFT column		H-section beam				Axial force ratio	
	Outside column (D x t)	Inside column (D x t)	Outside beam		Inside beam		Outside (N/N_u)	Inside (N/N_u)
			I_x	Z_P	I_x	Z_P		
1	603x12.6	725x15.1	3.88	1.10	2.64	0.82	0.21	0.25
2	600x12.5	721x15.0	3.78	1.08	2.57	0.81	0.20	0.24
3	596x12.4	716x14.9	3.65	1.05	2.48	0.79	0.19	0.22
4	591x12.3	710x14.8	3.49	1.02	2.38	0.76	0.17	0.21
5	585x12.2	702x14.6	3.31	0.98	2.26	0.73	0.16	0.20
6	577x12.0	692x14.4	3.10	0.93	2.11	0.70	0.15	0.18
7	568x11.8	681x14.2	2.87	0.88	1.96	0.66	0.14	0.17
8	557x11.6	668x13.9	2.62	0.82	1.78	0.61	0.13	0.16
9	544x11.3	652x13.6	2.34	0.75	1.59	0.56	0.12	0.15
10	528x11.0	634x13.2	2.04	0.68	1.39	0.51	0.11	0.13
11	510x10.6	612x12.7	1.72	0.60	1.17	0.45	0.10	0.12
12	487x10.2	585x12.2	1.38	0.51	0.94	0.38	0.09	0.10
13	459x 9.6	551x11.5	1.02	0.40	0.69	0.30	0.07	0.09
14	421x 8.8	505x10.5	0.64	0.28	0.44	0.21	0.06	0.07
15	363x 7.6	437x 9.1	0.64	0.28	0.44	0.21	0.04	0.05

D: Diameter of steel tube (mm), t: Thickness of steel tube (mm),
I_x: Moment of inertia of H-section beam (x10^9mm^4), Z_P: Plastic modulus of H-section beam (x10^7mm^3)

Table-2 F7-3 Frame (σ_c=60N/mm^2)

Story	Steel tube of CFT column		H-section beam				Axial force ratio	
	Outside column (D x t)	Inside column (D x t)	Outside beam		Inside beam		Outside (N/N_u)	Inside (N/N_u)
			I_{xu}	Z_P	I_x	Z_P		
1	536x11.2	644x13.4	2.26	0.73	1.54	0.55	0.12	0.15
2	526x11.0	631x13.2	2.03	0.68	1.39	0.51	0.11	0.13
3	512x10.7	614x12.8	1.76	0.61	1.20	0.46	0.10	0.12
4	492x10.2	590x12.3	1.43	0.52	0.98	0.39	0.08	0.10
5	464x 9.7	557x11.6	1.06	0.42	0.72	0.31	0.07	0.09
6	425x 8.9	511x10.6	0.66	0.29	0.45	0.22	0.56	0.07
7	363x 7.6	437x 9.1	0.66	0.29	0.45	0.22	0.38	0.05

D: Diameter of steel tube (mm), t: Thickness of steel tube (mm),
I_x: Moment of inertia of H-section beam (x10^9mm^4), Z_P: Plastic modulus of H-section beam (x10^7mm^3)

4.2 Designed CFT frames

15-story 3-bay frames (F15-3 frame) and 7-story 3-bay frames (F7-3 frame) are designed under the conditions mentioned above and the condition that any section of steel tube are available. In order to design the realistic CFT frame, the following frame sizes and materials are used in the design conditions. The height of every story is 4.0 m and the span lengths of outer span and inner span are 8.0 m and 6.0 m respectively. The weight of each story is 2000KN. The yield stress (σ_y) and tensile strength (σ_u) of steel tube and H-section beam are σ_y=340N/mm^2, σ_u=440N/mm^2. The compression strength of concrete (σ_c) is σ_c=60N/mm^2. The designed CFT frames are shown in Table-1 and Table-2.

5. SEISMIC RESPONSE AND COLLAPSE OF CFT FRAME

5.1 Dynamic collapse of CFT frame under extremely strong artificial ground motion

In order to calculate the dynamic collapse of CFT frame, the extremely strong artificial ground motion (ART NS & UD) is used as the input motion of CFT frame. The characteristics and intensity of it are explained by the response spectra in Fig.10 comparing with the strong ground motion JMA-KOBE NS & UD (1995) recorded in Kobe. In Fig.10 NS and UD mean the horizontal and vertical components of the ground motion respectively.

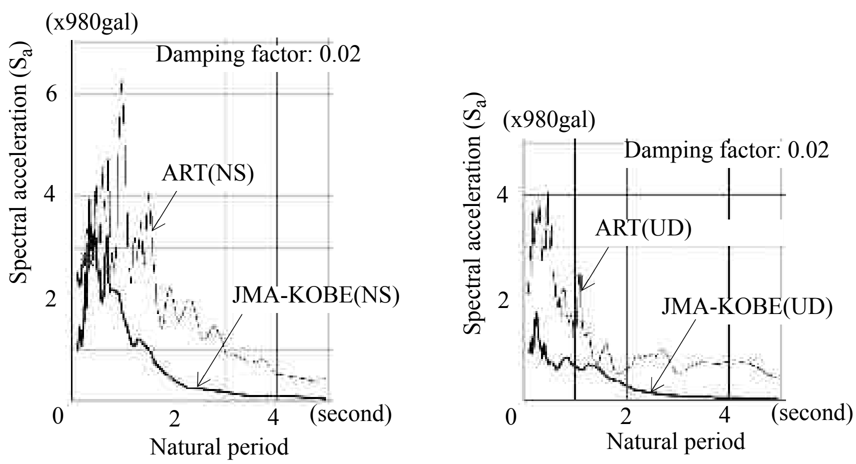

Fig.10 Seismic response spectra of the artificial ground motion (ART NS & UD) and the recorded strong ground motion (JMA-KOBE NS & UD)

To analyze dynamic collapse of CFT frame, the following conditions for calculation are also used.

i) After the crack of steel tube of CFT column or H-section beam, the restoring force and the stiffness of the member is fully and linearly lost in 0.1 second.

ii) In falling down process of frame, the collision force between the upper and lower rigid panels of beam-column connection is given by the compression load-deformation relation obtained from the stub-column tests of CFT member.

The calculated seismic response of CFT frame under the artificial ground motion ART NS & UD are shown in Fig.11-Fig.15. In Fig.11 the dynamic collapse behaviors of CFT frame are expressed by the seismic response deformations of frame in every 4 seconds. The numbers in the figure show the time elapsed from the beginning of seismic ground motion. We can see in Fig.11 the complicated response deformation of CFT frame which varies the shape of deformation in every seconds.

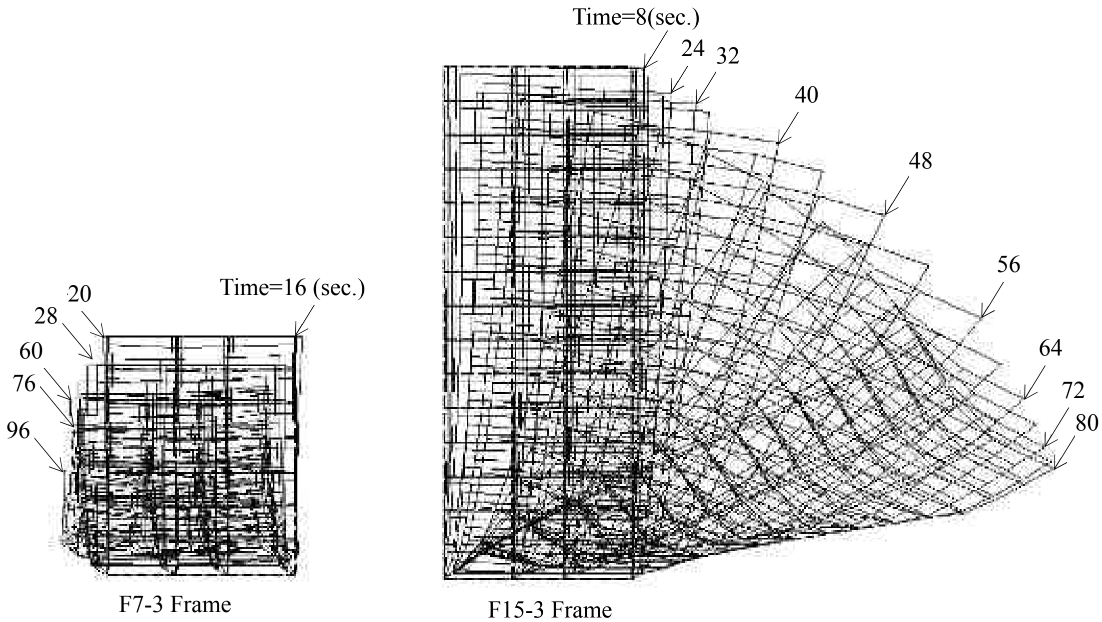

Fig.11 Dynamic collapse of frame under extremely strong ground motion (ART NS & UD)

From the calculation of seismic response of CFT frame under the extremely strong ground motion, the following collapse behaviors and falling down process are obtained.

i) When CFT frame is subjected to strong ground motion, at first the steel tube of CFT column buckles locally near the column end. The local buckling is closely related to the crack of steel tube. This behavior is shown in Fig.12 which is the time history of damage factor of the first story columns. After the steel tube of CFT column buckles locally (D_{lb}=1.0), the increase of the crack damage ratio (D_{cr}) becomes remarkable and continues to increase monotonically until the steel tube cracks (D_{cr}=1.0).

ii) After the first crack of CFT column, the steel tube crack appears successively in other CFT columns of the same story. At the same time the steel tubes of CFT column in other stories also buckle locally.

iii) When the steel tube cracks and the restoring force of CFT column is lost suddenly, the CFT frame begins to fall down locally. Soon after the crack of CFT column, the H-section beam also begins to crack in some middle stories. After the local failure of frame in the lower stories the collapse of CFT frame develops repeating the collision between the upper and the lower rigid panels of beam-column connection and the shape of response deformation of frame changes complicatedly with time as shown in Fig.11.

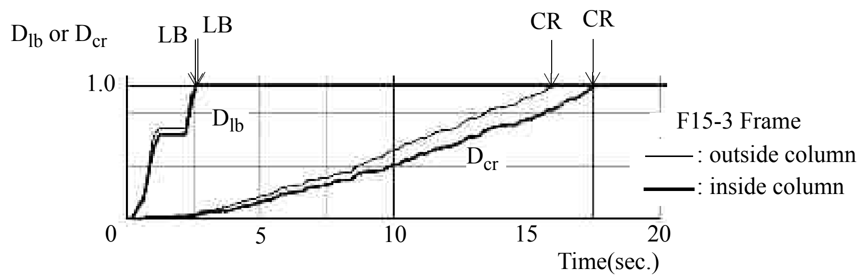

Fig.12 Time history of damage factors (LB: Local buckling, CR: Steel tube crack)

The restoring force characteristics of CFT column under the extremely strong artificial ground motion are shown in Fig.13-Fig.15. In the seismic response of CFT frame under extremely strong ground motion, the varying axial force of column is remarkable and effects not only on the local buckling or steel tube crack of CFT column but also on the bending restoring force of CFT column. To explain the effect of the varying axial force of column (N), the N-M relations of CFT column are shown in Fig.13. In the figure the numerically analyzed seismic response of CFT frame is expressed by the dots and the real lines show the N-M_u relation obtained by the generalized superposed strength method[1)-3)]. The axial force ratio shown by the dashed lines are the initial axial force ratio of CFT column (N_o/N_u).

We can see the remarkable change of axial force especially in the outside column which makes the ultimate bending strength of CFT column deteriorate extremely. From this behavior it is shown that the varying axial force of column can not be neglected in seismic response analysis under strong ground motion.

.

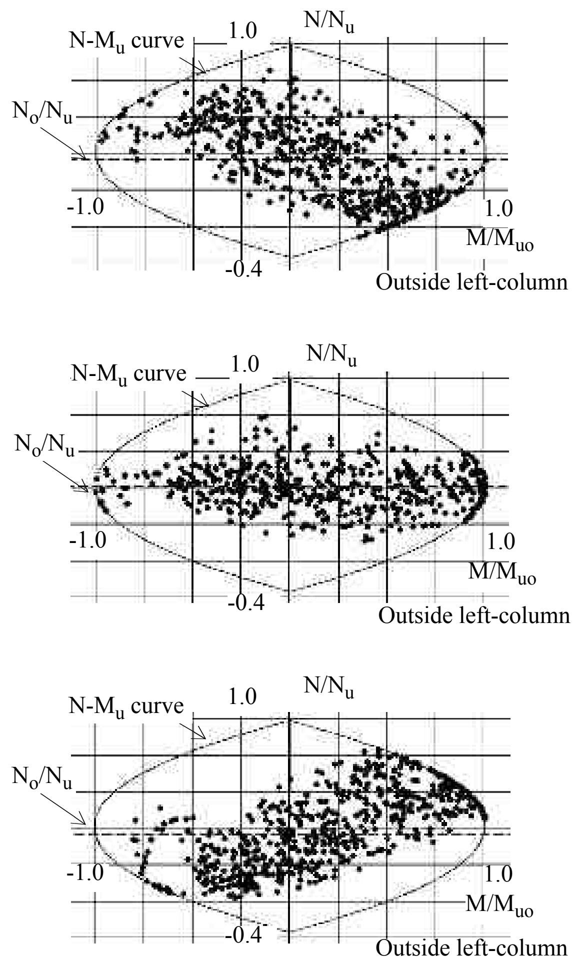

Fig.13 N-M relationships of the first story CFT-column (F15-3 Frame)
(N_o: initial axial force, M_{uo}: ultimate bending strength under N_o)

The varying axial forces of CFT column are also shown in Fig.14. In this figure the relations between the varying axial force and the deformation angle of CFT column are expressed. The dashed lines in this figure show the initial axial force (N_o). According to these figures, the axial force of the outside column extremely varies and the relation between the axial force and deformation of CFT column is very complicated.

The hysteretic bending restoring force effected by the varying axial force in the seismic response is expressed by the load-deformation relation in Fig.15. To make it clear that the varying axial force effects on the bending restoring force significantly, the load-deformation relations under the initial constant axial force (N_o) are shown by the thin lines in Fig.15. From the difference between the thick line and the thin line, we can see that the bending restoring force of CFT column is effected extremely by the varying axial force and its shape of load-deformation relation becomes to be very complicated.

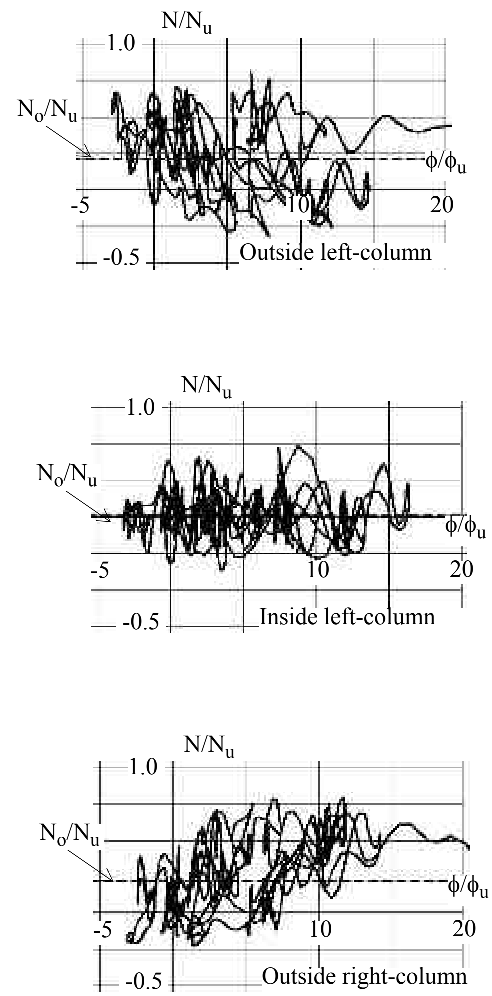

Fig.14 Varying axial force of the first story CFT-column (F15-3 Frame)

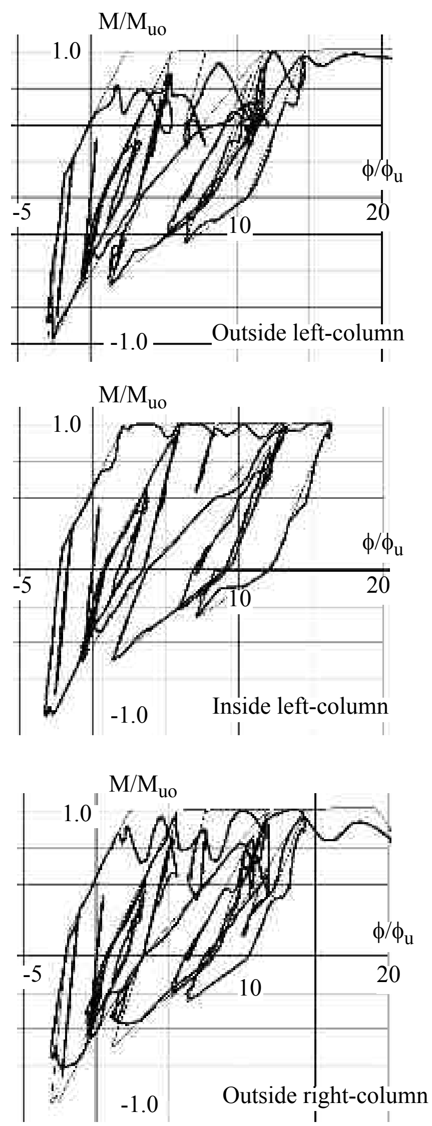

Fig.15 Bending restoringl force of the first story CFT-column (F15-3 Frame)

From these calculated results it is pointed out that the hysteretic bending force and axial force of CFT column under strong seismic load are very complicated and they can not be approximated by the widely used simple restoring force model like the Bi-linear model and the Tri-linear model which do not include the effect of varying axial force. On the other hand the proposed non-dimensional restoring force model of CFT column, which uses the ultimate bending strength at every instance (M_u) to exclude the effect of varying axial force, can predict well the complicated restoring force of CFT column under remarkably varying axial force.

5.2 Seismic response of CFT frame under recorded strong ground motion

The effects of the local buckling damage and the steel tube crack damage on the seismic response and collapse behavior of CFT frame under extremely strong artificial ground motion have been investigated in the former section. Under recorded strong ground motion, how they work on the seismic response of CFT frame is investigated in this section.

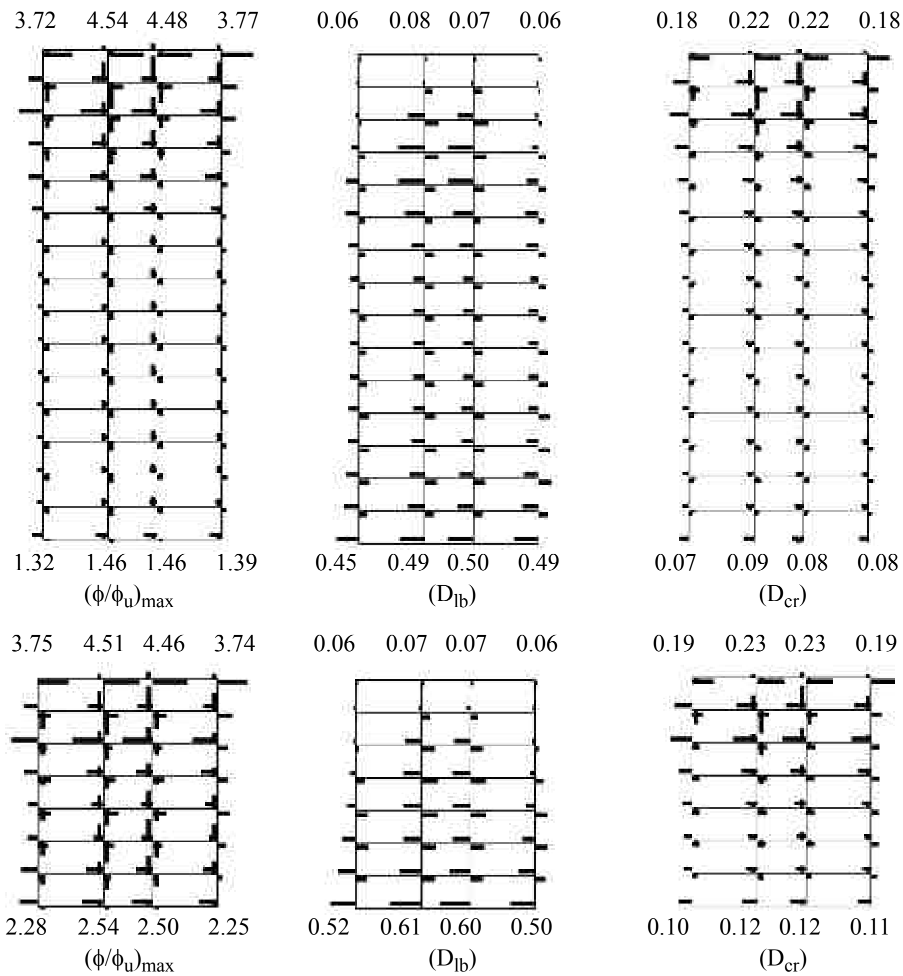

Fig.16 Damage distribution of CFT-frame under recorded strong ground motion (F15-3 Frame and F7-3 Frame under JMA-KOBE NS & UD)

The seismic responses of CFT frame under the JMA-KOBE NS & UD (1995) are calculated by the proposed dynamic collapse analysis method and shown in Fig.16-Fig.17. In Fig.16 there are the damage distributions in the CFT frame expressed by the maximum plastic deformation factor $(\phi/\phi_u)_{max}$, the local buckling damage ratio of steel tube (D_{lb}) and the crack damage ratio of steel tube and H-section beam (D_{cr}).

The CFT frames are designed according to the ideal design conditions of the column over design factor and the story-shear strength distribution. From the time history of the maximum damage ratios shown in Fig.17, the earthquake resistant capacity of the CFT frame seems to be sufficiently enough. But the damage concentrations and distributions are quite different among them as shown in Fig.16. From this reason the seismic response under strong ground motion is required to be analyzed numerically by the precise analysis method. The proposed dynamic collapse method can calculate the complicated restoring force characteristics under varying axial force and the large seismic response deformation of CFT frame in relation with the fracture failure of steel tube column and H-section beam. From this point of view the presented analysis method is useful as the tool of the earthquake resistant design and to apply to the seismic response and collapse analysis.

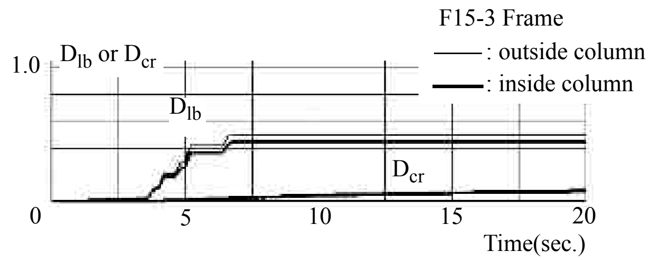

Fig.17 Time history of the maximum damage factors
(F15-3 Frame under JMA-KOBE NS & UD)

6. CONCLUSION

By the use of the local buckling damage of steel tube and the crack damages of CFT column and H-section beam, the dynamic collapse analysis method of CFT frame under extremely strong seismic load has been obtained.

From the numerical analysis of CFT frame carried out by the proposed analysis method, it is ascertained that the presented analysis method is useful to calculate the dynamic collapse behavior of CFT frame. It is also shown that the dynamic collapse of CFT frame is related directly to the local buckling and the crack of CFT column and H-section beam whose effects can be expressed by the damage factors (D_{lb}, D_{cr}). Accordingly the damage factors are the important design factors to decide the ultimate earthquake resistant capacity of CFT frame based on the collapse of frame.

REFERENCES

1) Saisho,M. and Goto,K., “Restoring Force Model of Concrete Filled Steel Tube Column under Seismic Load“, Proceedings of 6th Pacific Structural Steel Conference (PSSC2001), Vol.1, 2001.10., pp.453-458. (Beijing, China)
2) Saisho,M. and Matsuyama,T., “Restoring Force Characteristics and Model of Concrete Filled Steel-Tube Column“, Proceedings of the 12th World Conference on Earthquake Engineering (New Zealand), Paper No.1090, 2000.1.
3) Mitsunari,K. and Saisho,M., “Ultimate Strength and Plastic Deformation Capacity of CFT Beam-Column Subjected to Dynamic Load”, Proceedings of the 11th World Conference on Earthquake Engineering (Mexico), Paper No.414, 1996.6.
4) Clough, R.W. and Johnston, S.B., “Effect of Stiffness Degradation on Earthquake Ductility Requirements”, Proceedings of Japan Earthquake Engineering Symposium 1966, Oct.,1966, pp.227-232. (Tokyo, Japan)
5) Saisho,M., Kato,M. and Gao,S., “Local Buckling of CFT-Column under Seismic Load”, Proceedings of the 13th World Conference on Earthquake Engineering (Canada), Paper No.2614, 2004.8.
6) Dowling, N.E.,(1993), ”Mechanical Behavior of Materials”, Prentice Hall.

7) Saisho,M., “Seismic Response and Collapse of Concrete Filled Steel Tube Frame under Extremely Strong Ground Motion“, Proceedings of 6th Pacific Structural Steel Conference (PSSC2001), Vol.1, 2001.10., pp.441-446. (Beijing, China)